Astronomy & Astrophysics

Extragalactic globular clusters in the near infrared

IV. Quantifying the age structure using Monte-Carlo simulations

M. Hempel and M. Kissler-Patig

European Southern Observatory, Karl-Schwarzschild-Str. 2, 85748 Garching, Germany
e-mail: [mhempel,mkissler]@eso.org

Abstract. In previous papers of the series, we used a combination of optical and near-infrared colours to derive constrains on the relative age structure in globular cluster systems. Here, we present the details, strength and limitations of our method based on Monte-Carlo simulations of colour–colour diagrams and cumulative age distributions. The simulations are based on general informations about the globular cluster systems (e.g. colour-ranges, the number ratios between sub-populations) and the different single stellar population models (SSP's) which are used to derive relative ages. For both the modeled systems and the observed globular cluster systems we derive the cumulative age distribution and introduce two parameters to define it, the so-called 50% age and the result of the reduced χ^2 test of the comparison between models and observations. The method was tested successfully on several systems and allowed to reveal significant intermediate age populations in two of them.

Key words. galaxies: photometry – galaxies: star clusters

1. Introduction

Globular cluster systems have been extensively used in the last decade to interpret the formation and evolution histories of early-type galaxies (see for example Geisler et al. 2002 and Kissler-Patig 2003). A key question remains the origin of the multiple globular cluster sub-populations observed within most (if not all) individual galaxies. The metal-poor, halo sub-populations appear very uniform and are most probably linked to star cluster formation in the early structures of the universe (e.g. Ashman et al. 1994; Burgarella et al. 2001). However, the metal-rich sub-populations are less likely to be homogeneous in age and/or metallicity, as nicely seen e.g. in the sample of Kundu et al. (2001a,b) and might contain information on the more recent epochs of star formation in the galaxies. While certainly a large fraction of metal-rich globular clusters investigated so far is old (e.g. Puzia et al. 1999), the existence of large intermediate-age globular cluster populations has not been excluded yet and was actually shown to exist in at least some galaxies (e.g. Goudfrooij 2001; Puzia et al. 2002; Hempel et al. 2003).

This latter fact is closely related to one of the most important open questions in galaxy formation and evolution, namely whether galaxies formed the vast majority of their stars at early epochs, or whether a significant fraction of the stars originated from more recent events, such as dissipational mergers

(e.g. Kennicutt 1998; Renzini 1999; Renzini & Cimatti 1999; Schweizer 2000 and references therein).

The study of globular clusters in order to determine the major star formation epochs presents several advantages over the study of the diffuse galaxy light. Indeed- several age populations can be hidden in the diffuse light of the host galaxy (e.g. Larsen et al. 2003). Globular clusters on the other side represent single stellar populations, their stars sharing the same metallicity and the same age. The existence of sub-populations of globular clusters gives henceforth a stronger indication for different star formation epochs. Since the prediction and first discovery of multiple globular cluster sub-populations in early-type galaxies by Ashman & Zepf (1992, see also Zepf & Ashman 1993) their colour distributions have been investigated extensively. Various studies, e.g. by Gebhardt & Kissler-Patig (1999) and Kundu & Whitmore (2001a,b) have shown that bimodal colour distributions in elliptical galaxies are common. The exact interpretation, however, is hindered by the age-metallicity degeneracy of broad band colours (Worthey 1994).

Our group uses combined optical- and near infrared photometry (Kissler-Patig et al. 2002; Puzia et al. 2002; Hempel et al. 2003; hereafter cited as Papers I–III) to overcome this obstacle and partly lift this degeneracy. In Paper III, we showed how, using Single Stellar Population (SSP) models and the corresponding model isochrones, (e.g. by Bruzual & Charlot 2000; Vazdekis 1999; Maraston 2001) photometric studies of globular cluster systems can be used to derive their age distributions.

In this paper we present the details of our method, investigate the capability of photometric studies to detect globular cluster sub-populations of different ages within the metal-rich sub-population and the accuracy with which we can derive their relative ages.

The paper is organized as follows: in Sect. 2 we will describe our method of simulating colour–colour diagrams for globular cluster systems. Section 3 shows how these artificial distributions are compared to the observed data via their cumulative age distributions. Caveats and uncertainties of the method are presented in Sect. 4, first results and our conclusions are given in Sects. 5 and 6.

2. Modeling of colour distributions

2.1. Overview of the method

The basic idea of our approach is best described by a question: how would a colour–colour diagram of a globular cluster system look like if it was indeed *formed in two or more distinguishable star formation events*? We decided to model different cases and compare these to our data (Fig. 1, see also Paper III).

Originally, our ambition was a direct detection of the different globular cluster sub-populations in a given galaxy in our data (colour–colour diagrams) by comparing observed colour distributions with simulations following SSP models. This, however, turned out to be too difficult with non-converging solutions. Indeed- for the direct comparison of observed and simulated colour–colour diagrams we applied a two-dimensional Kolmogorov-Smirnov test (Press et al. 1992). However we had to consider a number of parameters which are included in our observations but difficult to include in the simulations, e.g. completeness limits, photometric error with high enough accuracy to still disentangle in 2 dimensions the parameters of interest (age, number ratios of the different populations). In Sect. 3 we describe our alternative, 1-dimensional approach via the cumulative age distribution.

At this stage we do not address the question of what actually ignited the cluster formation and are working with the final observed colour distribution only. Also, at this point, we stay with the assumption of two major star formation events and a first generation age of 15 Gyr out of convenience. The latter does not play a major role since we are interested in relative ages only. Further, if we take into account the age uncertainty of the model isochrone in the age range between 10 and 15 Gyr our assumption is still reasonable with respect to the new WMAP results giving a maximum age of the universe of 13.7 Gyr ± 0.2 Gyr (e.g. Bennett et al. 2003). We will also present results for NGC 5846 assuming the old population of age 10 Gyr in Sect. 5.1.

The basic principle is thus to input a number of properties for the two sub-populations to model (see next section), use a Monte-Carlo approach to model the distribution of the first colour, determine the second colour with the help of SSP's, construct a cumulative age distribution from this artificial two-colour diagram and compare the latter to its observed counterpart. These steps are repeated for various input variables that
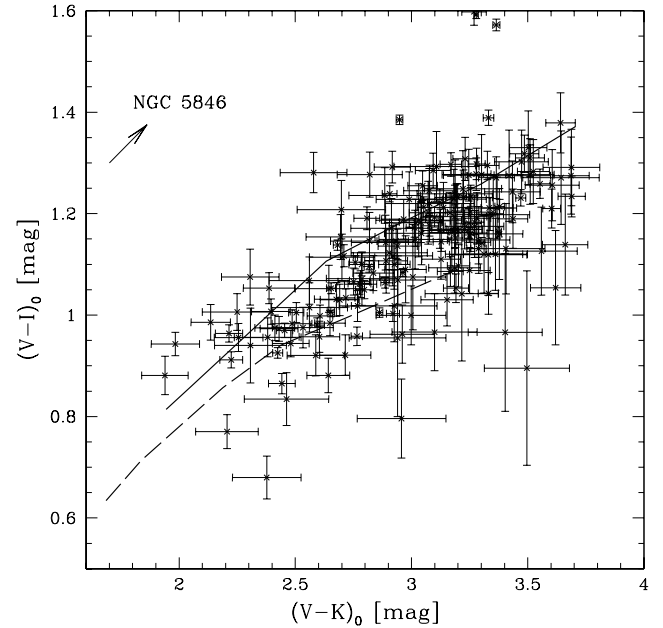

Fig. 1. Colour–colour diagram for the NGC 5846 globular cluster system. The solid and dashed line mark the 15 Gyr and 2 Gyr isochrone respectively following the Bruzual & Charlot SSP model (Bruzual & Charlot 2000).

scan the two parameter space (size of the second populations, age of the second population).

To illustrate the method, we use data presented in Paper III: we model colour–colour diagrams, $(V - I)$ vs. $(V - K)$, for a template globular cluster systems corresponding to the one of NGC 5846. This is a favorable example given the relatively large number of objects with VIK colours (188 globular clusters for the complete sample, when no limits for photometric errors, colour or limiting magnitudes are applied). In Sect. 4, we will also illustrate the caveats for smaller samples and the possibility of contamination.

An important note is that we are interested in the age structure of the metal-rich population only. We assume the *blue* $(2.0 \leq (V - K) \leq 2.7)$ population to consist of *old* objects only (in NGC 5846 43 clusters were assigned to the metal-poor population), and model exclusively the red $(2.7 \leq (V - K) \leq 3.8)$ colour range. We generate for our example case in total 120 metal-rich objects, split into an *old* and *intermediate age* population.

2.2. Input parameters to the simulation

Several input parameters get fixed with respect to the observed distribution.

- **the total number of metal-rich objects**, in our example we have 120 metal-rich globular cluster candidates and simulate individual colour distributions with that number of objects;
- **the primary colour range to be modeled**, in our template $(V - K)$ is used as primary colour in the range $2.7 < (V - K) < 3.8$. The lower limit is driven by the observed gap
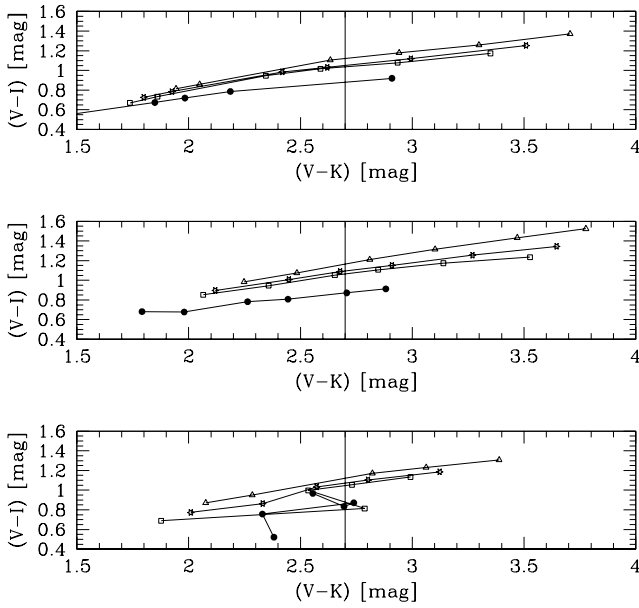
Fig. 2. Comparison between the SSP model isochrones given by Bruzual & Charlot (2000) (*upper panel*), by Vazdekis (1999) (*middle panel*) and Maraston (2001) (*lower panel*). Different symbols mark the 1 Gyr (solid circles), 3 Gyr (open squares), 5 Gyr (open stars) and 15 Gyr (open triangles) isochrones. The solid line at $(V - K) = 2.7$ marks boundary between **blue** and **red** objects (see Sect. 2.4).

Fig. 3. Least square fit of model isochrones given by Bruzual & Charlot (2000) (*left*), Vazdekis (1999) (*center*) and Maraston (2001) (*right*). Various isochrones are marked with solid squares (1 Gyr), open stars (3 Gyr), solid circles (5 Gyr), solid triangles (10 Gyr) and asterisks (15 Gyr).

between blue and red sub-populations, the upper limit encloses metallicities of up to twice solar at the highest ages, but excludes redder contaminating galaxies;

– **the SSP model** to be used in order to associate, for a given age, the secondary colour (in our case $(V - I)$) to each primary colour point;

– **the observed error distribution in the primary colour** which is used to randomly "smear" the primary colour after calculating the secondary colour;

– **the observed error distribution in the secondary colour** which is used to randomly "smear" the secondary colour.

For each study of a particular data set these fixed parameters can be chosen such as to mimic closely the observed data. In addition to these fixed parameters two variable input parameters are of interest: how many young clusters are present, and what is their age?

2.3. Variables of the simulation

Our scientific goal is to investigate *i)* whether a second, intermediate-age population is present in the metal-rich sub-population; and if so *ii)* what is the most likely age of the population and *iii)* what is its importance in number of clusters relative to the old metal-rich population. Thus, we explore the parameter space span by the two latter properties. To do so, each set of simulations is performed for a pair of these variables:

– **the relative number ratio of the old with respect to the intermediate age sub-population**. We vary the ratio of both populations between populations composed
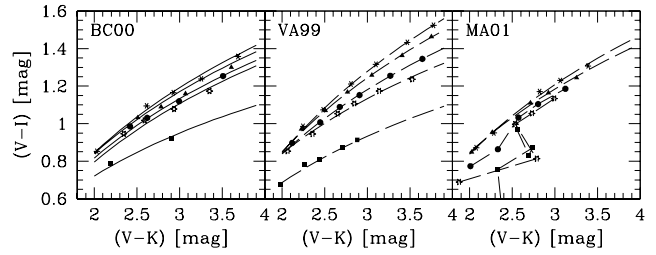
of 100% 15 Gyr old clusters (no younger sub-population present) to 100% young objects, in 10% increments;

– **the age of the second population** for which we modeled the cases of 1, 2, 3, 5, 7, and 10 Gyr.

Thus, simulations are preformed for each of the 66 possible pairs of variables. This leads to 66 master models which get compared to the observed data.

2.4. Monte-Carlo simulation to get a set of primary colours

For each individual simulation, we start by creating an artificial globular cluster samples in our primary colour. We populated the two $(V - K)$ colour intervals assigned to a **"blue"** and a **"red"** sub-population with an fixed number of objects. Hereby we assume a random distribution within this range. A second run of simulations using a Gaussian colour distribution in both populations did not lead to significantly different results than the once obtained for randomly distributed objects. Given the lack of physical support for Gaussian colour distributions, we stay with the simplest case: a pure random distribution.

2.5. Determination of the second colour and observational errors

The importance of using different SSP models, e.g. by Bruzual & Charlot (2000, hereafter named BC00), Vazdekis (1999, hereafter named VA99) or Maraston et al. (2001, hereafter named MA01) for our modeling becomes clear, if we compare the corresponding isochrones. In Fig. 2 the isochrones for a 1, 3, 5, 10 and 15 Gyr old SSP are shown following the model by Bruzual & Charlot (2000), Vazdekis (1999) and Maraston (2001). Especially in the red $(V - K)$ colour range we find a significant discrepancy for the corresponding $(V - I)$, resulting in a model dependency of the derived ages. Therefore we will apply different models in the age dating.

The next step in the simulation is the parametrisation of the model isochrones. A least square fit of $(V - I)$ as a logarithmic function of $(V - K)$ in the form $(V - I) = A \cdot \ln(V - K) + B$, as shown in Fig. 3, gives us a set of parameter A and B for all SSP models. Unfortunately the Maraston isochrones for SSP's
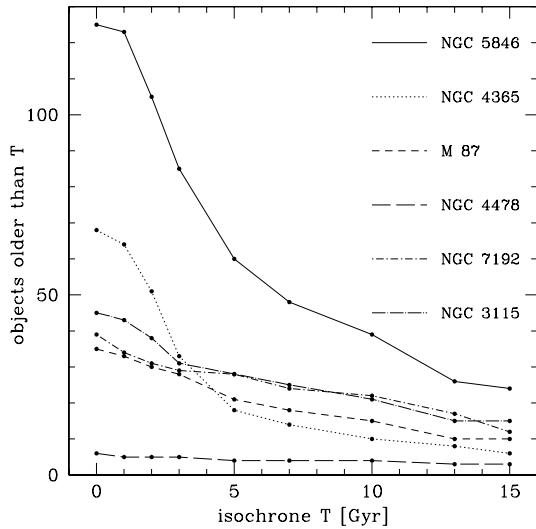
Fig. 4. Cumulative age distribution in the globular cluster systems of NGC 5846, NGC 4365, NGC 7192, NGC 3115, NGC 4478 and M 87.

in the lower age range (less than 5 Gyr) allow no simple parametrisation. We therefore decided to postpone the work with this specific model. The relations were used to calculate the *secondary* colour $(V - I)$ for each assumed age population. We generated colour–colour diagrams for globular cluster systems consisting of an old (15 Gyr) population and a second one, as explained in Sect. 2.3. Each simulation will therefore create the $(V - I)$ vs. $(V - K)$ colour–colour diagram for a mixed population of globular clusters. Finally both colours $(V - K)$ and $(V - I)$ were smeared with up to 3σ photometric error, taken from the NGC 5846 observed error catalog. In a last step, an artificial catalog with the two colours and their 1σ error is created. The final outcome of this process is the colour–colour distribution $(V - I) \pm \Delta(V - I)$ vs. $(V - K) \pm \Delta(V - K)$ for six age combinations and eleven number ratios. We generated 1000 models for each set of model parameters. The final product, the cumulative age distribution (see Sect. 3.1) to be compared with the observations, was determined as the statistical mean of the distribution of these 1000 models.

As we can see in Fig. 3, the isochrones for various SSP models (e.g. Bruzual & Charlot; Vazdekis & Maraston) differ strongly. Nevertheless there is no quality argument (Vazdekis et al. 1996) behind our choice of BC00 and VA99. Since Bruzual & Charlot provide models for the largest variety of ages and metallicities we started our modeling program using parametrised BC00 isochrones (Fig. 3, left panel). VA99 has been added later to test our method for model dependence. The latter will be discussed in Sect. 5. Both models assume a Salpeter IMF.

3. Quantifying the age structure

3.1. Cumulative age distribution

Photometric errors, which might become rather substantial in combined optical and near-infrared photometry, contribute

largely to the uncertainty in age determination. Comparing our limiting photometric error of 0.15 mag and the colour difference in $(V - I)$ for SSP's which differ in age by at least 1 Gyr (see Fig. 3), we conclude that not only absolute ages are out of reach but also an age resolution more accurate than several Gyr. Nevertheless- our major goal is the detection of cluster sub-populations in order to give evidence for various major star formation events during the evolution of the galaxy. Since we assume this events to be caused by merging or accretion, likely but not very frequent events, age differences larger than 5 Gyr are to be expected. The cumulative age distribution (see Fig. 4) which we derive is only based on the object density in the colour–colour diagram with respect to the isochrones and is less sensitive to photometric errors compared to a direct age determination. Since the result will refer to the globular cluster system the size of the sample becomes important, as we will show in a later section (see Sect. 4.2).

The derivation of the cumulative age distribution is a straight forward procedure and is identical for observed and simulated samples. Each object was assigned to an age older than X if its $(V - I)$ colour was found to be redder than for the isochrone of that age. The model isochrones for different ages at low $(V - K)$ values are hard to distinguish and the $(V - I)$ colour of a specific isochrone depends only weakly on $(V - K)$ in the red- colour regime. Therefore we set a lower colour limit (see also Paper III) for $(V - K)$ of ≤ 2.6, corresponding roughly to a metallicity of [Fe/H] ~ -0.7 dex, slightly above the split between metal poor and metal rich clusters in galaxies.

The upper limit was set to $(V - K) \geq 3.6$, which agrees with the upper $(V - K)$ limit in our NGC 5846 sample. The age distributions are normalised with respect to the total number of objects within $2.6 \leq (V - K) \leq 3.6$. The notation 0 Gyr in the cumulative age distribution refers to the total number of objects (per definition all objects are "older" than 0 Gyr).

3.2. The comparison with observed data: χ^2 test

The relative size of globular cluster sub-populations provides some constrains for the galaxy formation scenario. In Ashman & Zepf (1992) the efficiencies of the globular cluster formation in dependency of the environment (cluster galaxies or "normal" elliptical galaxies) and the amount of available gas are compared and found to differ significantly. Therefore we are interested in the ratio between possible globular cluster sub-populations. Since the globular cluster samples are limited to the inner most region of the globular cluster systems this result will only answer the question whether there is a second population and to which extend we can constrain its age and relative size compared to an old population.

To quantify the age structure we compare the cumulative age distributions of the observed and modeled data sets. By using a reduced χ^2 test we find the best fitting model for the observed system.

Due to the age uncertainty of the models, the 3σ scatter in colour allowed in the model, and to the photometric error in the observations, we expect a certain degeneracy in
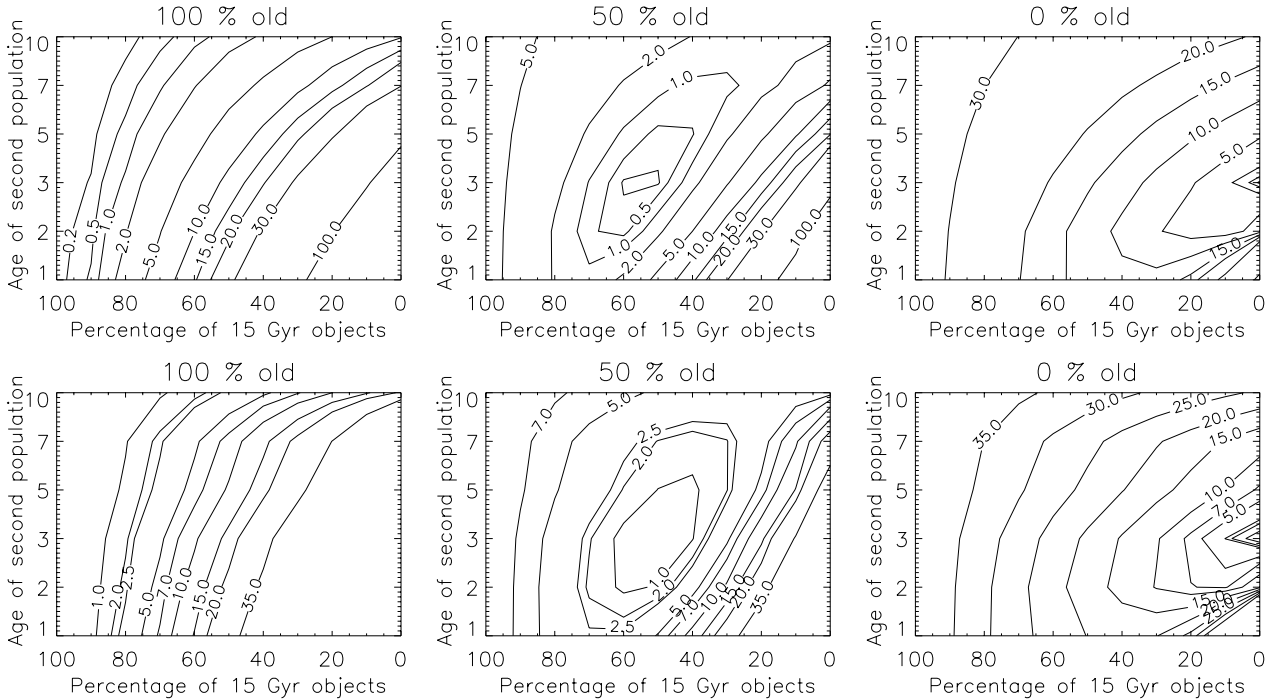
Fig. 5. Self-consistency test: age distributions of individual model systems compared to the complete model set. The result of the χ^2 test are shown as σ-contours. For this test we use the model of a purely 15 Gyr old population (*left*), a 15 Gyr + 3 Gyr mixture (*middle*) and a purely 3 Gyr old population (*right*). As expected the result for the purely old population is much more uncertain than for the other two, allowing as best fitting model also mixed populations. The upper plots show the result for the BC00 model and the lower plots the VA99 models. The different spread of the isochrones (see Fig. 2) results in different uncertainties.

the age/ratio combinations. Nevertheless we are able to constrain the age as well as the ratio between the two populations. This was tested by comparing the age distribution for three selected models with the complete model set. The χ^2 test should pinpoint the model which was chosen in the first place. In Fig. 5 we show the result for the χ^2 test for models of a 100% 15 Gyr, a 50% 15 Gyr + 50% 3 Gyr and a 100% 3 Gyr population respectively. As we can see in the plots the χ^2 tests return the model parameters we chose as the best fit, including an uncertainty in age and number ratio. Due to the different $(V - I)$ colour range for BC00 (upper panel) and VA99 (lower panel) SSP isochrones the result of the χ^2 test differ slightly.

3.3. Comparison of different SSP models

Before we start comparing our results based on the SSP models by Bruzual & Charlot (Charlot & Bruzual 1991; Bruzual & Charlot 1993) and by Vazdekis (Vazdekis et al. 1996) we want to make the point that our choice is by no means to interpret as judgment on the various models. As Vazdekis et al. (1996) pointed out there is, despite the different modeling procedure, little difference in the quality of the various models, which mostly differ in the covered range of metallicity and age and in accuracy of the physical input parameter. The SSP models by Bruzual & Charlot are based on the Padova library from 1994. The newer version, based on the Padova 2000 library, is used in the latest SSP model by Bruzual & Charlot, but not recommended by the authors (see Bruzual & Charlot 2003). Details can be found in Bruzual & Charlot (2003). For more

information about the VA99 model we refer to Vazdekis et al. (1996). The essential difference to the BC00 models being the application of empirical stellar libraries whereas Bruzual & Charlot make use of the libraries by Lejeune (e.g. Lejeune et al. 1997). The latter are based on the stellar atmospheres derived by Kurucz (e.g. Kurucz 1992). We would like to stress again that we do NOT attempt to judge the quality of different models but use them to discuss our method with respect to model uncertainties. Our choice of the BC00 and VA99 model is therefore highly subjective and mostly driven by the typical error is introduced by parametrising the model isochrones for calculating the secondary colour (as explained in Sect. 2.4). In the future, we intend to replace the parametrised by linear interpolated secondary colours in order to reduce this error. In the discussion of our results (see Sect. 5.1, Fig. 18) we will present first results based on this modification.

The smaller spread in $(V - I)$ for BC00 results in a finer scanning of the colour–colour diagram and gives therefore better results in the χ^2 test. For larger sample sizes (observed and simulated systems) this effect will become more and more negligible. We expect the strongest effect for the comparison of small observed systems (e.g. NGC 4478) with the relatively large (120 clusters) model systems (see Sect. 5).

4. Potential caveats

4.1. Contamination with background objects

Using colour distributions with respect to model isochrones is strongly affected not only by photometric errors but also
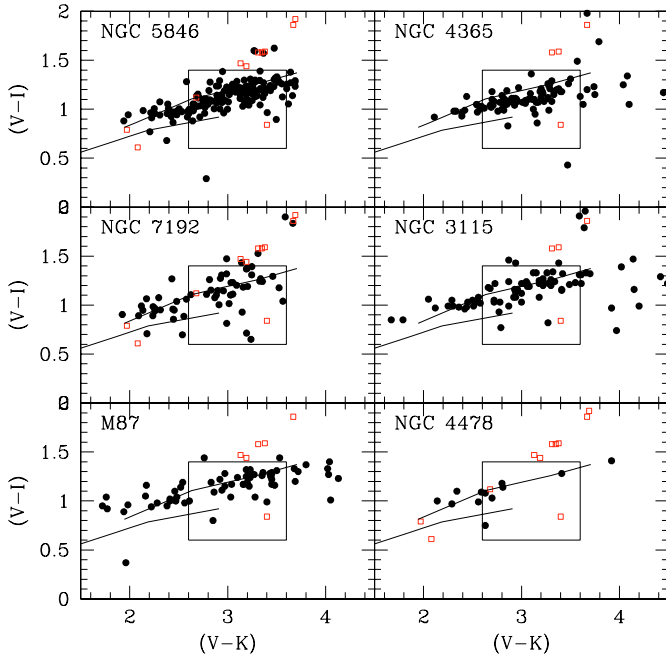
Fig. 6. Comparison of colour–colour diagrams for the globular cluster systems and the HDF-S. Globular clusters are marked by filled circles and HDF-S objects by open squares. The solid lines mark the 1 Gyr and 15 Gyr isochrone respectively, as given by Bruzual & Charlot (2000). The box marks the colour range used for determining the cumulative age distribution.
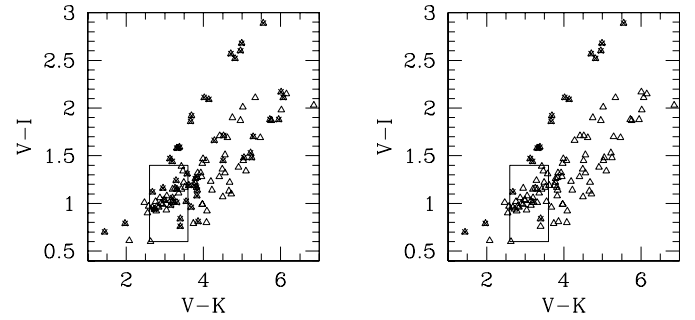

Fig. 7. Colour–colour diagram for the HDF-S sample ($K > 21.5$) before (triangles) and after (cross) applying shape parameter for selection. For selection the ellipticity (<0.2, left panel) and the star/galaxy classifier (>0.8, right panel) have been used. For final correction we choose a combination of photometric error, limiting magnitude and classifier. As in Fig. 6 the box indicates the colour limits.
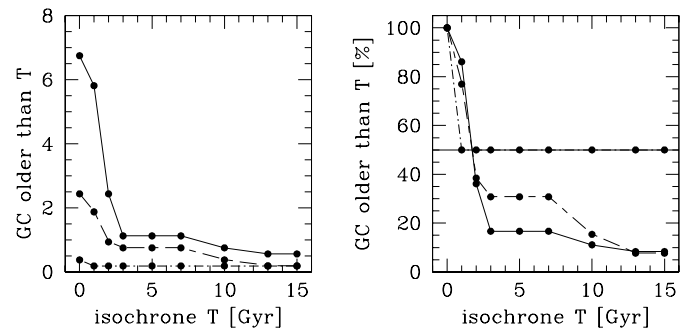

Fig. 8. Cumulative age distribution in the HDF-S sample (BC00) normalised to 1 arcmin^2 (*left*: absolute, *right*: relative). The solid line marks the result if only a error cut of 0.15 mag for all filters is applied. Applying an additional ellipticity limit (<0.2) results in a age distribution indicated by the dashed line. Using a combination of error cut and star/galaxy classifier (>0.8) given by SExtractor (Bertin & Arnout 1996) most background galaxies can be rejected from the data set (dotted-dashed line).

by false identification of objects. Within the red colour range, as it has been defined in Sect. 3.1, the contamination of our globular cluster sample by background galaxies and/or foreground stars has to be considered. In the red ($V - K$) colour range these objects are most likely unresolved background galaxies. Assuming their random distribution on the sky we use the Hubble-Deep-Field South, available from the archive of ST-ECF[1] as a representative background sample. We are well aware that a random distribution of background objects is only the case in a first approximation (Roche et al. 1993; Infante & Pritchet 1995; Maller et al. 2003).

In Fig. 6 we compare the colour–colour diagrams for observed systems, taken from Papers I–III, with the background sample, to which the same selection criteria as to the cluster sample have been applied, i.e. limits for the photometric error, the limiting K-magnitude and the colour cuts for ($V - K$) and ($V - I$) (marked by the box). Additionally the HDF objects have been selected using the SExtractor star/galaxy classifier as shape parameter. For comparison, the colour–colour diagram for the HDF-S sample is given in Fig. 7 using only error cuts and limiting magnitude (symbol: △) or including ellipticity (left panel) and classifier (right panel) as well. The latter was applied to our observed data sets.

To account for the background contamination we applied different correction procedures. For all of them we determined the age distribution for the HDF-S objects (Fig. 8), using the procedure given in Sect. 3.1. Due to the different limiting K-band magnitude in the observed systems the age distribution

of the HDF was determined for each globular cluster system separately.

In the first trial (see Paper III) we corrected age distribution for the observed systems following a worst case scenario. Hereby we subtracted the number of HDF-S objects in each age interval (older than "X") from the number of objects found in the observed systems. This works only in cluster samples much larger than the HDF-S sample, but will fail in less numerous systems, e.g. NGC 3115, NGC 7192 and NGC 4478.

In a second run the correction was applied to the colour–colour distribution in the observational data. Before counting objects with respect to a given model isochrone we rejected all objects in the observed sample if a HDF-S object was found with a difference in ($V - K$) and ($V - I$) < 0.1 mag. This links each contaminating object directly to an observed object. Differences in the colour distribution are therefore included. Observed systems with a large number of objects are handicapped in this procedure if a background object is found in the vicinity of several objects in the observed cluster

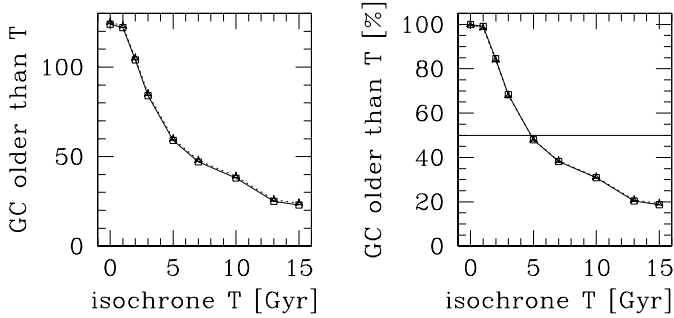[1] www.stecf.org/hstprogrammes/ISAAC

Fig. 9. Cumulative age distribution in NGC 5846. The left panel shows the cumulative age distribution before (triangles, dotted line) and after (open squares, solid line) correction for contamination applying an error cut as well as a selection by star/galaxy classifier. In the right panel the distribution has been normalised to the total number of objects in the sample after correction (125 objects within the colour limits). The age dating was done following the SSP models by Bruzual & Charlot.

Fig. 10. Cumulative age distribution (using BC00) in the globular cluster systems observed so far. The left panel shows the relative distribution without background correction. The correction applied in the right panel follows the procedure given in the previous section.

system. Additionally no informations about the shape of the background objects are included yet. The globular cluster samples are selected for point sources whether the HDF objects include as well (even mostly) extended objects.

The final most realistic correction for background objects was therefore done by setting limits for the photometric error in all bands (0.15 mag) and the parameter "classifier" given by SExtractor. Due to the extraordinary depth of the HDF images the classifier has been set to a limit of 0.8, which should be sufficient to reject most of the extended objects. As an example the correction effect in the cumulative age distribution for NGC 5846 is shown in Fig. 9. In the left panel the absolute number of objects per age bin [0 Gyr, T] before and after correction is shown. The right panel gives the relative age distribution for both sets. In case of NGC 5846 we find only 7 HDF-S objects within the selected colour range, which results in an insignificant correction. Nevertheless – this changes drastically for smaller cluster samples or in case of deeper imaging of the globular cluster systems.

In our comparison of cumulative age distributions we work with globular cluster systems of very different sizes, NGC 5846 and NGC 4365 being the largest with a total number of about 190 clusters, and on the other side NGC 4478 with only 21 GCs, most of them excluded from the age distribution by the colour cuts. As described in Sect. 2 we used NGC 5846 as template system and have therefore to check whether the age distribution and the resulting χ^2 test depend on the size of the observed globular cluster systems. In Fig. 10 we show the cumulative age distribution for all observed globular cluster systems before and after correcting for background contamination. Due to the selection criteria for background objects the correction effect is rather small, except for NGC 4478, where the remaining cluster set might not allow statistical stable results (see next section).

4.2. Stability of contamination correction

In the previous section we opened the discussion to which extend the sample size affects the final result. In the competition
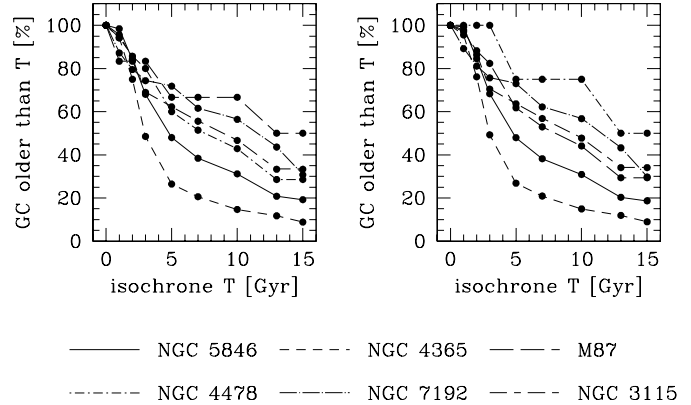
between spectroscopy and photometry toward relative age dating this becomes even more important, the sample size being the advantage of photometry. But what is the minimum size of the cluster system, for which the scattering in the data (e.g. due to photometric errors) becomes negligible in the age distribution? To answer this question we modeled the colour–colour diagram of a mixed cluster population (50% 15 Gyr old objects and 50% 3 Gyr old objects). The age distributions for systems between 10 and 200 objects are shown in Fig. 11. We find that in systems with less than 60 objects the age distribution varies significantly. With respect to Sect. 3.3 we find this effect being even stronger if the VA99 model isochrones are used.

In order to minimise the scattering effect in the simulated cluster system we generated 1000 models and work with the statistical mean of the age distribution (see Sect. 2.4). Still the sample size for the models has to be considered. In Fig. 12 we compare the age distribution for models consisting of either 100% old objects or a 50%: 50% mix of 15 Gyr and 3 Gyr old globular clusters in a set of only 10, 60 or 120 clusters. The error bars give the standard deviation of the object counts in the 1000 models. In systems with only 10 objects the age distribution for a mixed population and a purely old system are, within the error limits, indistinguishable. In slightly larger samples (e.g. 60 objects) the age distributions of a purely old and a mixed population overlap in the older age bins. The result would be multiple findings of best fitting models (see Sect. 4.3). As a last point we want to mention that our primary assumption of a random distribution in $(V - K)$ becomes critical for small samples.

4.3. Is there a significant intermediate age cluster population?

In Fig. 13 we show the result of the reduced χ^2 test for finding a specific input model within our complete set of 66 models of varying sample sizes for the BC00 model. In contrast to the simulations the age distribution in the observed globular cluster systems represents a single sample still subject
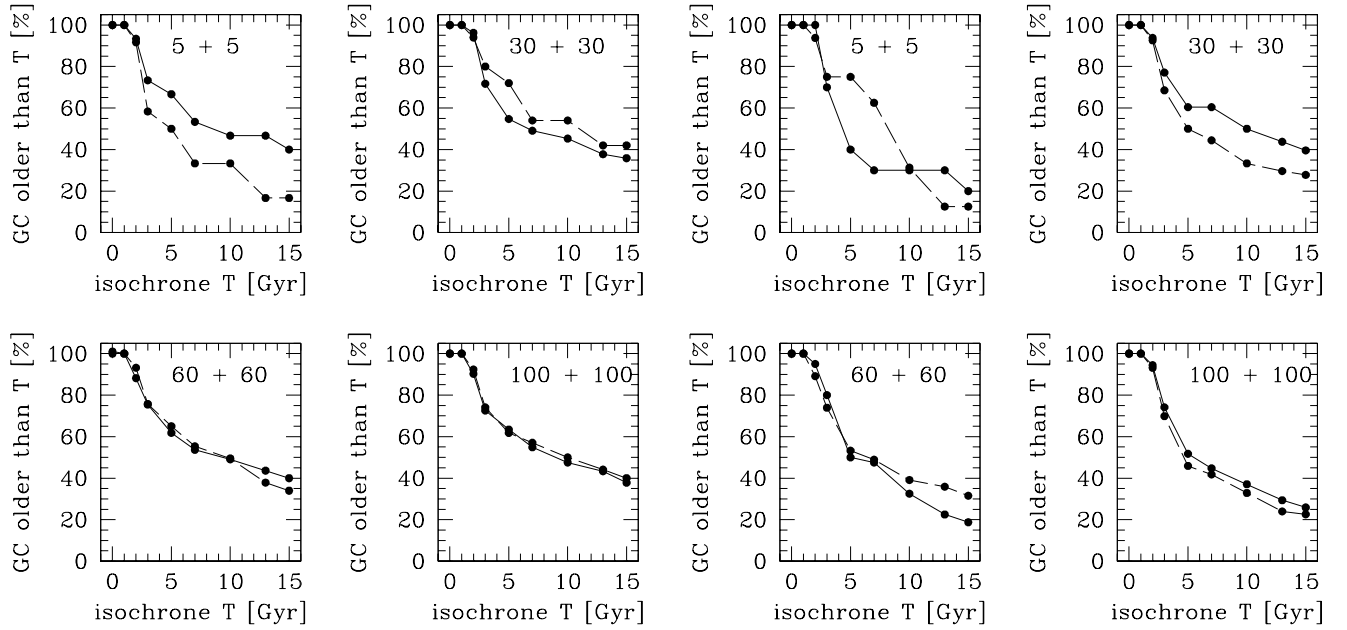
Fig. 11. Cumulative age distribution for modeled samples, consisting of a different number of objects but assuming a constant mixture of old and intermediate age objects (50%:50%). The results are shown for the BC00 (*left*) and VA99 (*right*) SSP models respectively. Each panel shows the age distribution for two out of six different runs of modeling.
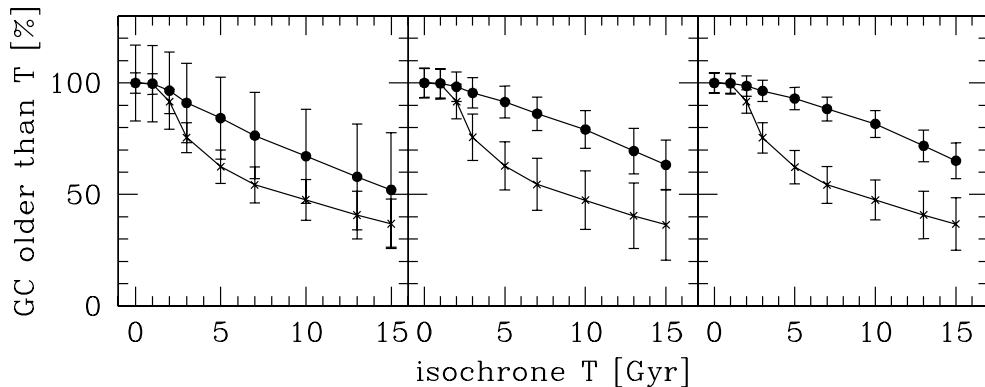

Fig. 12. Cumulative age distribution (using BC00) derived for models of 10, 60 and 120 objects respectively. To show the importance of large number of objects we show the standard deviation of the counting rate. The models were created for a purely 15 Gyr old population (solid circles) and a 50%:50% mix (×) of 15 and 3 Gyr old objects.

to stochastic effects. In order to test the stability of our derived ages/number ratios for various sample sizes we compare the age distribution for six individual simulations (assuming the same model parameters but different sample sizes). The example shown here are based on the BC00 model. As we can see, we should be able to detect sub-populations, if their ages differ by several Gyr. Nevertheless, for small sample sets the results become quite unstable, i.e. the age of the young sub-population and the size ratio between both populations are more uncertain. Again- this is more important for the VA99 model, due to the steeper $(V - I)$ gradient of the isochrones. We also have to keep in mind that all the models were created based on our largest globular cluster system- NGC 5846 and we therefore expect the most reliable results for sample sets which are in size and colour range similar to NGC 5846. Special attention

has to be paid to NGC 4478, where the majority of objects is found in the blue colour range. In order to draw stricter conclusions about the red sub-populations the modeling parameters (size, $(V - K)$ colour range) have to be chosen with respect to the observed cluster system.

Although we have discussed the effect that unresolved background objects can have on the results, we are aware that we are at this point not able to offer a quantitative correction for each of the observed systems. Even if our final selection criteria (error cut and classifier) for background objects (see Sect. 4.1) are too strict – we do not expect contamination to play a major role in large globular cluster systems. Only the NGC 4478 (21 cluster in total) sample falls into the low number region where the stability of the χ^2 test is questionable.
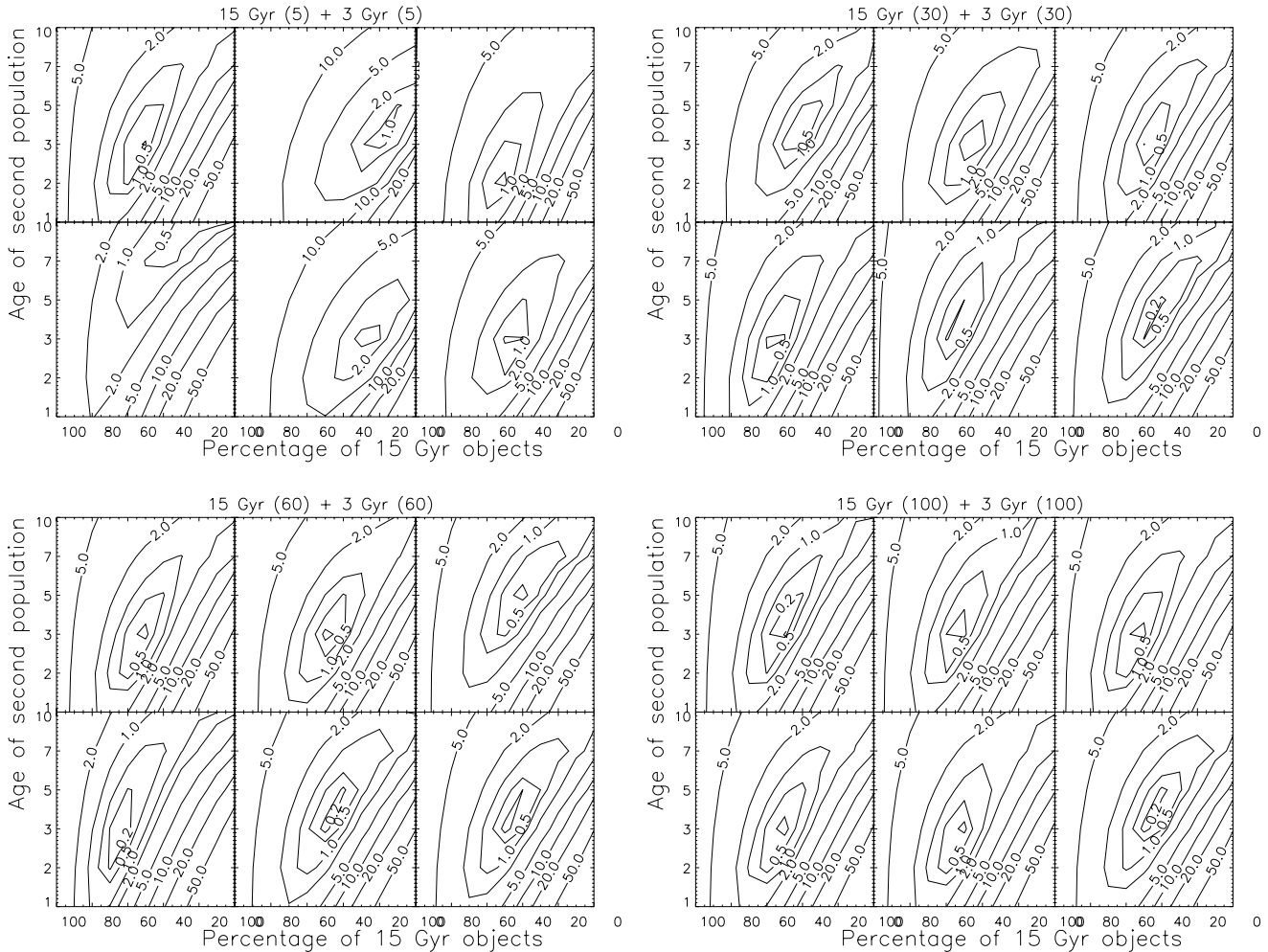
Fig. 13. Examples of the reduced χ^2 test (see Sect. 3.2) for different sample sizes (10, 60, 120 and 200 objects). The age distribution for a mixture of 50% 15 Gyr and 50% 3 Gyr old clusters (see Fig. 11) with the complete set of models are compared. On top of each plot the number of old and intermediate objects within the "red" population is given. We compare the results for six separate runs of modeling.

5. Results for observed systems

The goal of relative age dating via the cumulative age distribution is to find evidence for various major star formation events in elliptical galaxies and to constrain those in their age difference and importance for the galaxy evolution. To do so we compare two features of the age distribution, the so-called 50%-age and the result of an χ^2 test between simulated and observed globular cluster systems. The 50%-age is defined as the age at which the cumulative age distribution intersects with the 50% level. Figure 14 shows the cumulative age distribution for all globular cluster systems observed so far, using the SSP model by Bruzual & Charlot and Vazdekis, respectively.

If we compare this 50%-level age derived for the observed systems with the models (see Fig. 15) we find a significant model dependence. We will include this parameter in our discussion.

For NGC 5846 and NGC 4365 with large globular cluster systems we obtain consistent results, independently on the SSP model. The 50%-age of both systems agrees with the 50%-age derived for a mixed population, hosting a second cluster population at an age up to 5 Gyr. In M 87 the 50%-age

gives as well evidence for a second population with an age of ~7 Gyr. For NGC 7192, NGC 3115, NGC 4478 the results for the 50%-age are inconsistent and depend on the used SSP models. NGC 4478 is a exceptional case for this study. The observed globular cluster system is very small and consists of mostly metal-poor objects. Within the $(V - K)$ colour range we find only 3 clusters, which is not sufficient for our analysis.

As mentioned in Paper III our intention regarding the modeling was the possibility to make quantitative statements about the star formation history in various galaxies. In the next section we present the result of the comparison between the observed globular cluster systems and the Monte-Carlo simulations. We provide some limits on the age structure for 4 of the observed systems. As introduced in Sect. 4.3 we discuss the results in the light of their SSP model dependence, which seems to be predictable in a way that applying VA99 models results in slightly younger ages and requires a larger sample size.

5.1. NGC 5846 and NGC 4365

Spectroscopic (Larsen et al. 2003) and photometric (Papers II and III) results for NGC 5846 and NGC 4365 have shown that
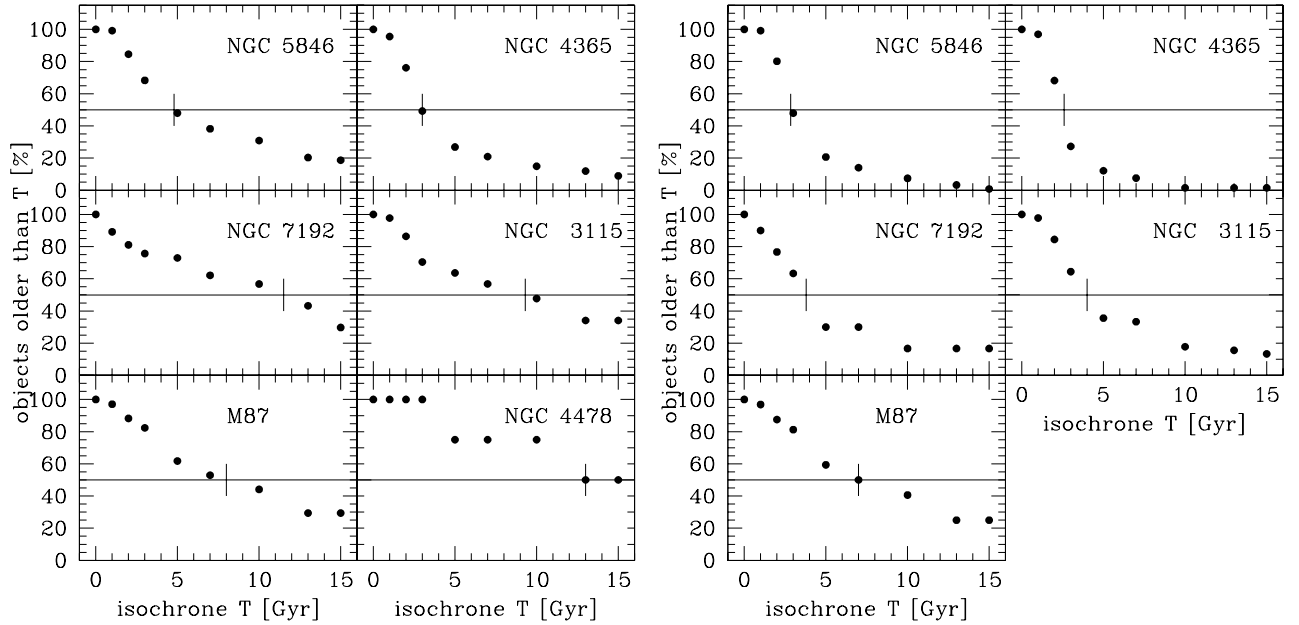
Fig. 14. Cumulative age distribution in the globular cluster systems using BC00 (*left*) and VA99 (*right*) SSP model isochrones. The samples are corrected for background contamination following the procedure given in Sect. 4.1. The horizontal line marks the 50% level and the vertical line its intersection with the derived age distribution.
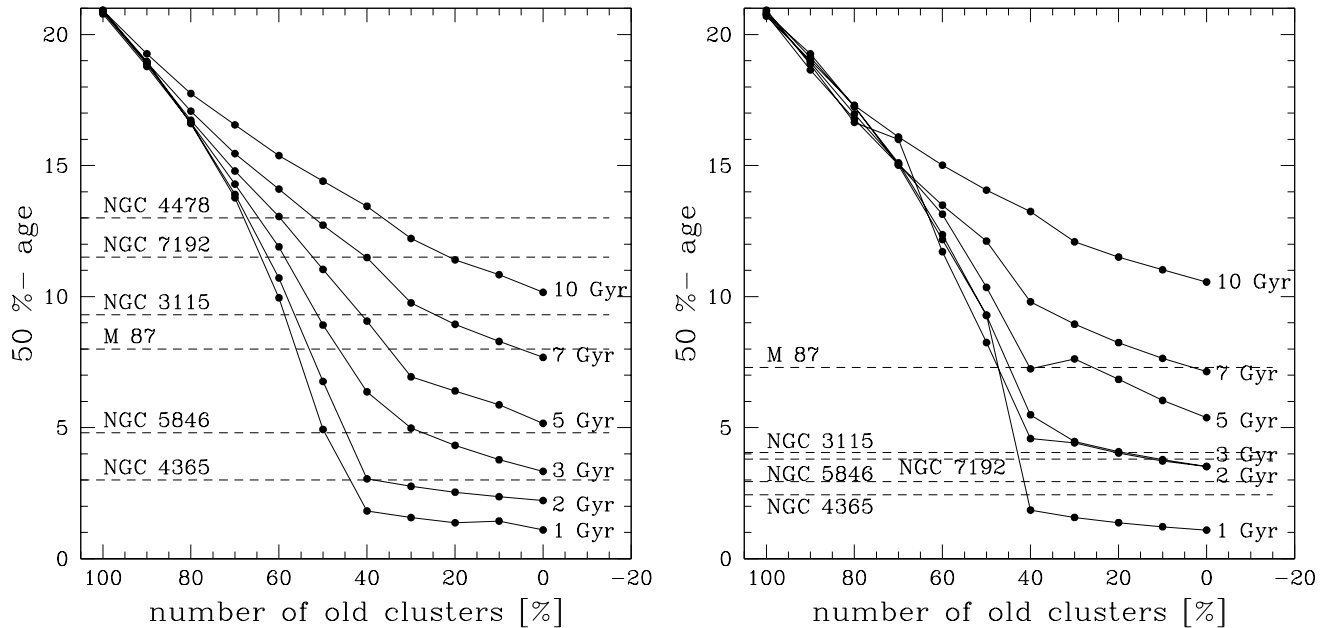

Fig. 15. We compare the 50%-age calculated by a best fit of the cumulative age distribution for observed and simulated systems using BC00 (*left*) and VA99 (*right*) SSP model isochrones. The x-axis gives the amount of 15 Gyr old objects within the model and the label on the right hand side the age of the intermediate age sub-population. The larger spread in (V − I) for VA99 isochrones results in a less reliable result for smaller samples. All systems have been corrected for background contamination.

both globular cluster systems host an intermediate age population indicating a second star formation period. In Fig. 16 we present the photometric and spectroscopic data for the globular clusters in NGC 4365, NGC 5846, NGC 7192 and NGC 3115 for which optical/ near-infrared photometric and spectroscopic data are available (33 objects). The left panel shows the

(V − I) vs. (V − K) colour–colour distribution of all clusters compared to the MA01 model isochrones. In the right panel the index measurements for H$_\beta$ and MgFe are compared with the SSP model by Thomas et al. (Thomas et al. 2003) and confirm the photometric age dating. The globular clusters assigned to an intermediate age are those found in NGC 4365 and NGC 5846.
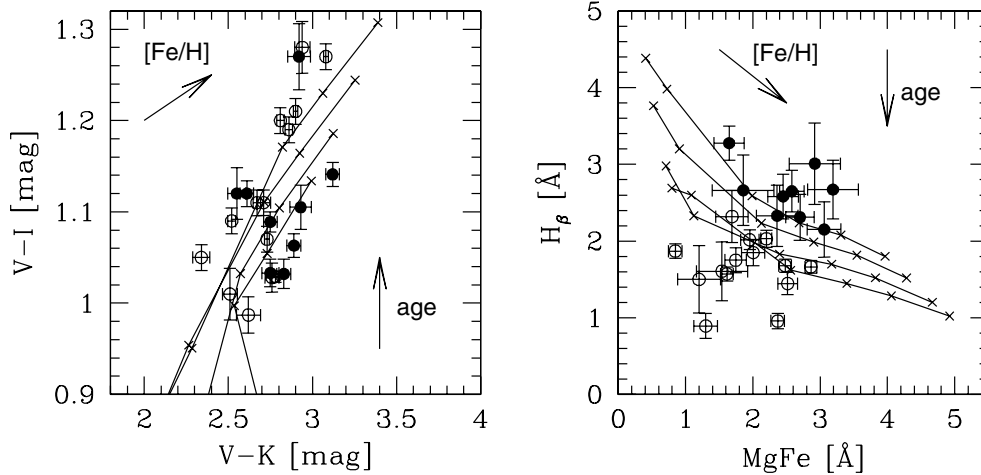
Fig. 16. *Left panel*: colour–colour diagram for globular clusters in 4 different galaxies. The model grid follows the Maraston (2001) SSP model isochrones (ages between 3 and 15 Gyr following the age-arrow). The metallicity ([Fe/H] between −2.25 and +0.35) increases in direction of the metallicity arrow. *Right panel*: comparison of index measurements with the models by Thomas et al. (2003) (age range: 3−15 Gyr, metallicity range: −2.25−+0.67). Objects with spectroscopic ages below 5 Gyr are shown by solid circles.

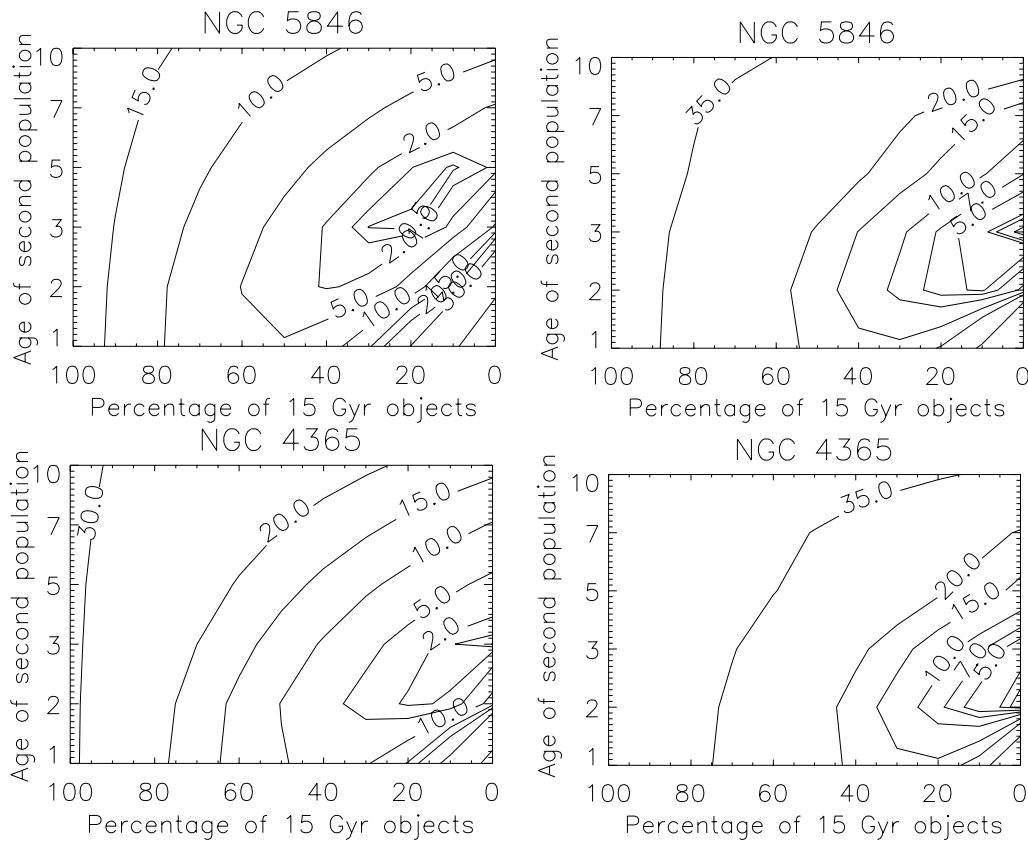**Fig. 17.** χ^2 test result for NGC 5846 (*upper*) and NGC 4365 (*lower*). The different levels represent the reduced χ^2 of the comparison between the age distribution in the observed systems and the various models. The correction for contamination following the procedure given in Sect. 4.1 has been applied. The left panels give the result following the BC00 models and the right panels following the VA99 models.
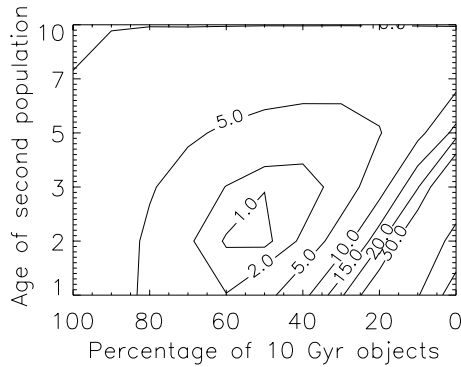
Fig. 18. Result of the χ^2 test comparing the age distribution in NGC 5846 with simulated systems assuming the *old* population being 10 Gyr old. As clearly seen the best fitting model still contains a much smaller, but still significant number of intermediate age objects.

Consequently we expect the 50%-age to show the best agreement with the value calculated for mixed populations as well as the best fitting model being a mixture of "old" and "intermediate" age globular clusters. For both SSP models we obtain 50%-ages below 5 Gyr the Vazdekis model giving slightly younger ages. Still the results are in good agreement with the value derived for models mixing an old population with globular clusters with ages up to 3 Gyr. The upper panels of Fig. 17 show the results of the χ^2 test for NGC 5846 and gives the highest agreement between the cluster sample and the models assuming a mixture of and old (15 Gyr) population and roughly up to 90% 3–5 Gyr old clusters. We will discuss this extremely large value, which we find for most of our target systems in Sect. 6. For NGC 4365 (Fig. 17, lower panels) we derive a mixture of 15 Gyr and 1–3 Gyr old objects with a higher content of intermediate age objects. The age range is in agreement with the spectroscopic results given by Larsen et al.(2003). Both observed cluster samples are relatively rich ($N_{\mathrm{NGC\ 5846}}$ and $N_{\mathrm{NGC\ 4365}}$ are in the range of 190) and the correction effect is relatively weak and, taking the stability tests into account as well (see Sect. 4.2), stable.

As mentioned in Sect. 2.1 the simulations are based on the assumption of an old population which is 15 Gyr old. We present one example to illustrate how the results will change in case of a 10 Gyr *old* population (see Fig. 18). Although the relative size of both populations changes considerably, as we would expect, the detection of an intermediate age population is confirmed and the relative ages of both populations do not change significantly. Moving from 15 to 10 Gyr, besides being driven by real physical arguments, also illustrates how our results would change if the SSP models are not perfectly calibrated.

5.2. M 87 and NGC 7192

With respect to the formation scenario for early-type galaxies we are interested in the environmental effect. Therefore our galaxy sample includes also cD galaxies (M 87) and rather isolated galaxies (NGC 7192). In both types of globular cluster

systems one wouldn't expect a second, younger globular cluster population (for M 87 see Jordán et al. 2002). This expectation is only met by the 50%-age derived for M 87. Using the Bruzual & Charlot model we estimate a 50%-age of 8 Gyr and for VA99 ~7 Gyr, both values being more consistent with models containing only a small population of somewhat younger objects. The fact that this result could not be confirmed by the χ^2 test (see Fig. 19) led us back to the problem of small sample sizes. As soon as we include the size of both globular cluster systems, 35 found for M 87 and 39 for NGC 7192 respectively, this inconsistency can be explained. Both systems are still not numerous enough to allow a meaningful analysis.

6. Discussion and conclusions

In this paper we describe our method of relative age dating in globular cluster systems using integrated photometry and constrain its suitability. The main emphasis is not the determination of ages with only small uncertainties, as it has been done in various papers by using spectroscopy for integrated light or globular clusters (e.g. Trager et al. 1998; Kuntschner 2000; Poggianti et al. 2001; Moore et al. 2002; Puzia et al. 2003), but to introduce a method to identify different age populations in large systems and to evaluate the importance of the underlying star formation events. From the results presented here we conclude that for large globular cluster sets integrated photometry is a suitable tool to search for sub-populations of globular clusters. The size of the young population appears excessively large when compared to the maximum allowed young population in the integrated light of these galaxies. Based on the fact that we study all globular cluster systems in the center of galaxies and assuming that intermediate clusters, formed during merger, settle down in the new center of gravity, our data will be biased toward these intermediate age objects. More observations covering regions more distant to the center of the host galaxies are necessary to overcome this bias effect. Yet, the bias alone is unlikely to explain the fraction >80% found in NGC 5846 and NGC 4365. Our example in Sect. 5.1, using an age of 10 Gyr for the old population, resulting in fractions close to 40% of young clusters, illustrates how the method is sensitive to this choice and/or proper SSP calibration. We conclude that our idealized SSP models probably still host uncertainties, especially do not take into account anything but age and metallicity, e.g. α/Fe varying abundance ratios etc. might play a role and introduce additional scatter or systematic error in the old population, driving our results to an interpretation of overly large young populations. These effects will be investigated in the future together with modelers, in particular the effect of α/Fe enhancement, as now incorporated into the models by Maraston & Thomas (Thomas et al. 2003; Maraston et al. 2003). Together with a modified calculation of the secondary colour (see Sect. 2.5) these are the next steps for improving our approach. For now the method is able to detect intermediate age populations, roughly constrain their age but most probably overestimates their importance. To lower the age uncertainty in the colour–colour distributions the observations will be extended into the blue wavelength region, e.g. by including the U-band. As shown in Fig. 20 ($U - I$) vs.

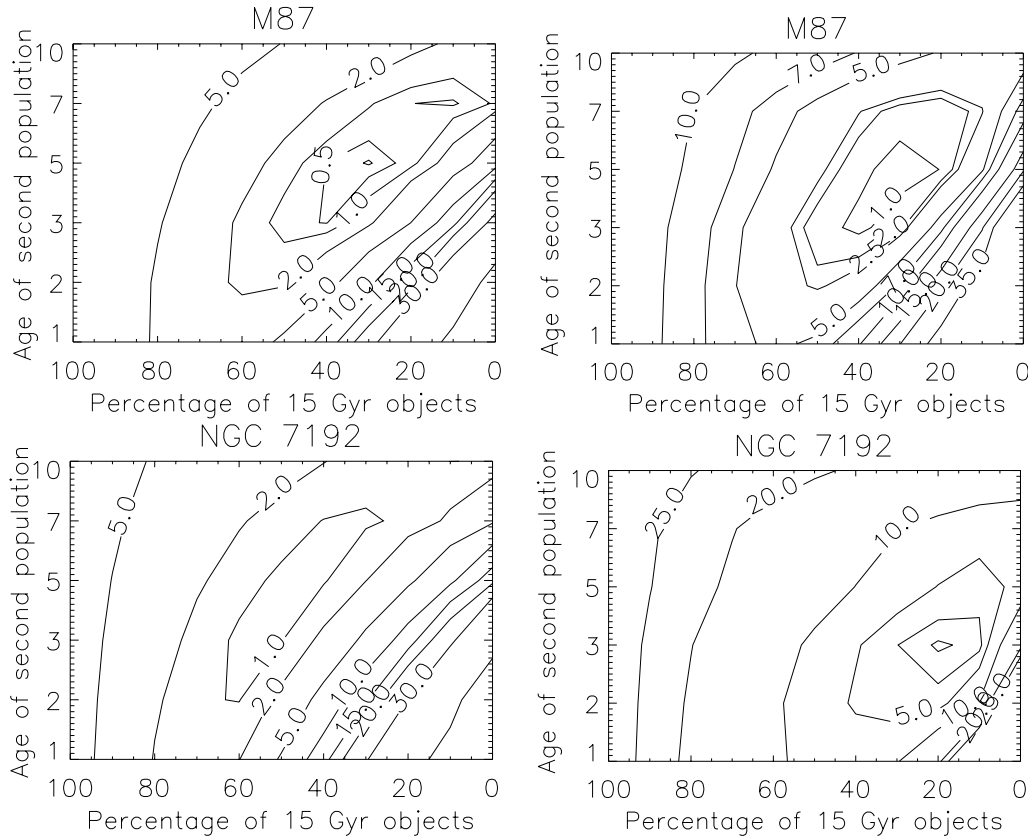**Fig. 19.** χ^2 test result for M 87 (*upper*) and NGC 7192 (*lower*). As in Fig. 17 the results for BC00 (*left panels*) and VA99 (*right panels*) are shown.
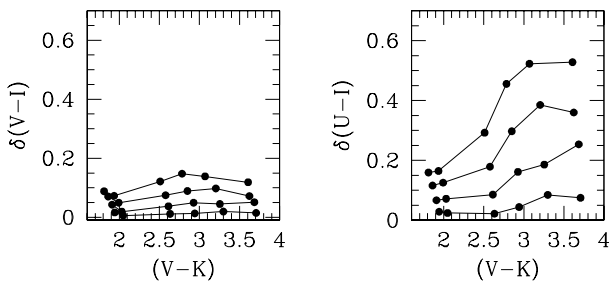

Fig. 20. Age resolution for SSP model isochrones by Bruzual & Charlot (Bruzual 2000) in $(V - I)$ vs. $(V - K)$ (*left panel*) and $(U - I)$ vs. $(V - K)$ (*right panel*) colour–colour diagrams. The age splitting in $(U - I)$ vs. $(V - K)$ plots is increased by a factor of 2 and will therefore result in a better age resolution. For direct comparison we chose an uniform scaling for both plots. The difference in $(V - I)$ and $(U - I)$, respectively, between a 15 Gyr model isochrone and the one for 13, 10, 7, and 5 Gyr (from bottom to top) is shown here.

$(V - K)$ colour–colour diagrams will result in a considerably larger age resolution.

References

Ashman, K. M., & Zepf, S. E. 1992, ApJ, 384, 50

Ashman, K. M., Bird, C. M., & Zepf, S. E. 1994, AJ, 108, 2348

Bennett, C. L., Halpern, M., Hinshaw, G., et al. 2003, ApJ, accepted

Bertin, E., & Arnout, S. 1996, A&AS, 117, 393B

Brodie, J. P. 2002, IAU Symp. Ser., 207, 218

Bruzual, G. A., & Charlot, S. 1993, ApJ, 405, 538

Bruzual, A. G. 2000, private communication

Bruzual, G., & Charlot, S. 2003, MNRAS, 344, 1000

Burgarella, D., Kissler-Patig, M., & Buat, V. 2001, AJ, 121, 2647

Charlot, S., & Bruzual, G. A. 1991, ApJ, 367, 126

Charlot, S., Worthey, G., & Bressan, A. 1996, AJ, 457, 625

de Grijs, R., Bastian, N., & Lamers, H. J. G. L. M. 2003, ApJ, 583, L17

Elmegreen, B. G., & Efremov, Y. N. 1997, ApJ, 480, 235

Forbes, D. A., Brodie, J. P., & Grillmair, C. J. 1997, AJ, 113, 1652

Forbes, D. A., & Forte, J. C. 2001, MNRAS, 322, 257

Gebhardt, K., & Kissler-Patig, M. 1999, AJ, 118, 1526

Geisler, D., Grebel, E. K., & Minniti, D. 2002, Extragalactic Star Clusters, IAU Symp., 207

Goudfrooij, P., Alonso, M. V., Maraston, C., et al. 2001, MNRAS, 328, 237

Harris, W. E. 1991, ARA&A, 29, 543

Harris, W. E. 2003, Extragalactic Globular Cluster Systems (Springer Verlag), ed. M. Kissler-Patig, ESO Astrophys. Symp., 317

Hempel, M., Hilker, M., Kissler-Patig, et al. 2003, A&A, 405, 487 (Paper III)

Infante, L., & Pritchet, C. J. 1995, AJ, 439, 565

Jordán, A., Côté, P., West, M. J., et al. 2002, ApJ, 576, L113

Kennicutt, R. C. 1998, in Galaxies:Interactions and Induced Star Formation, ed. D. Friedli, L. Martinet, & D. Pfenniger (Springer Verlag)

Kissler-Patig, M. 2000, RvMA, 13, 13

Kissler-Patig, M., Brodie, P. B., & Minniti, D. 2002, A&A, 391, 441 (Paper I)

Kissler-Patig, M. 2003, Extragalactic Globular Cluster Systems (Berlin: Springer Verlag)

Kundu, A., & Whitmore, B. C. 2001, AJ, 121, 2950

Kundu, A., & Whitmore, B. C. 2001, AJ, 122, 1251

Kuntschner, H. 2000, MNRAS, 315, 184

Kurucz, R. L. 1992, IAU Symp., 149, 225

Larsen, S. 2001, IAU Symp. Ser., 207

Larsen, S., Brodie, J. P., Beasley, M. A., et al. 2003, ApJ, 585, 767

Lejeune, Th., Cuisinier, F., & Buser, R. 1997, A&AS, 125, 229L

Maller, A. H., McIntosh, D. H., Katz, N., et al. 2003, ApJ, submitted [arXiv:astro-ph/0304005]

Maratson, C., Greggio, L., & Thomas, D. 2001, Ap&SS, 276, 893

Maraston, C., Greggio, L., Renzini, A., et al. 2003, A&A, 400, 823

Moore, S. A. W., Lucey, J. R., Kuntschner, H., et al. 2002, MNRAS, 336, 382

Poggianti, B. M., Bridges, T., Carter, D., et al. 2001, AJ, 563, 118

Press, W. E., Teukolsky, S. A., Vetterling, W. T., et al. 1992, Numerical Recipes in Fortran (Cambridge University Press)

Puzia, T. H., Kissler-Patig, M., Brodie, J. P., et al. 1999, AJ, 118, 2743

Puzia, T. H., Zepf, S. E., Kissler-Patig, et al. 2002, A&A, 391, 453 (Paper II)

Puzia, T. H., Kissler-Patig, M., Thomas, D., et al. 2003, A&A, in preparation

Renzini, A. 1999, in The formation of galactic Gulges, ed. Carollo, Ferguson, & Wyne (Cambridge University Press)

Renzini, A., & Cimatti, A. 1999, ASP Conf. Proc., 193, 312

Roche, N., Shanks, T., Metcalf, N., et al. 1993, MNRAS, 263, 360

Schweizer, F., Miller, B. W., Whitmore, B. C., et al. 1996, AJ, 112, 1839

Schweizer, F. 2000, Phil. Trans. R. Soc. Lond., Ser. A, 358, 2063

Thomas, D., Maraston, C., & Bender, R. 2003, MNRAS, 339, 897

Tinsley, B. M. 1972, ApJ, 179, 319

Toomre, A. 1977, in The Evolution of Galaxies and Stellar Populations, ed. V. Trimble, & R. B. Larson, 401

Trager, S. C., Worthey, G., & Faber, S. M. 1998, ApJS, 116, 1

Trager, S. C. 2003, in Carnegie Observatories Astrophys. Ser., 4 (Cambridge University Press)

Vazdekis, A., Casuso, E., Peletier, R. F., et al. 1996, ApJS, 106, 307

Vazdekis, A. 1999, ApJ, 513, 224

Worthey, G. 1994, ApJS, 95, 107